Neuron
Report

Necroptosis Drives Motor Neuron Death in Models of Both Sporadic and Familial ALS

Diane B. Re,[1,2,8] Virginia Le Verche,[1,2,8] Changhao Yu,[1,2] Mackenzie W. Amoroso,[1,2,5,6,9] Kristin A. Politi,[1,2] Sudarshan Phani,[1,2] Burcin Ikiz,[1,2] Lucas Hoffmann,[1] Martijn Koolen,[1,7] Tetsuya Nagata,[1,2] Dimitra Papadimitriou,[1,2] Peter Nagy,[1,2] Hiroshi Mitsumoto,[1,3] Shingo Kariya,[1,2] Hynek Wichterle,[1,2,4,6] Christopher E. Henderson,[1,2,3,4,5,6] and Serge Przedborski[1,2,3,*]

[1]Center for Motor Neuron Biology and Disease, the Columbia Translational Neuroscience Initiative, and the Columbia Stem Cell Initiative
[2]Department of Pathology and Cell Biology
[3]Department of Neurology
[4]Department of Neuroscience
[5]Department of Rehabilitation and Regenerative Medicine
Columbia University, New York, NY 10032, USA
[6]Project A.L.S./Jenifer Estess Laboratory for Stem Cell Research, New York, NY 10032, USA
[7]Academisch Medisch Centrum, University of Amsterdam, 1105 AZ Amsterdam, the Netherlands
[8]These authors contributed equally to this work
[9]Present address: Department of Molecular and Cellular Biology, Harvard University, Cambridge, MA 02138, USA
*Correspondence: sp30@columbia.edu
http://dx.doi.org/10.1016/j.neuron.2014.01.011

SUMMARY

Most cases of neurodegenerative diseases are sporadic, hindering the use of genetic mouse models to analyze disease mechanisms. Focusing on the motor neuron (MN) disease amyotrophic lateral sclerosis (ALS), we therefore devised a fully humanized coculture model composed of human adult primary sporadic ALS (sALS) astrocytes and human embryonic stem-cell-derived MNs. The model reproduces the cardinal features of human ALS: sALS astrocytes, but not those from control patients, trigger selective death of MNs. The mechanisms underlying this non-cell-autonomous toxicity were investigated in both astrocytes and MNs. Although causal in familial ALS (fALS), SOD1 does not contribute to the toxicity of sALS astrocytes. Death of MNs triggered by either sALS or fALS astrocytes occurs through necroptosis, a form of programmed necrosis involving receptor-interacting protein 1 and the mixed lineage kinase domain-like protein. The necroptotic pathway therefore constitutes a potential therapeutic target for this incurable disease.

INTRODUCTION

Amyotrophic lateral sclerosis (ALS) is an incurable, adult-onset paralytic disorder that presents mainly as a sporadic condition (sALS), i.e., it occurs in absence of any evidence of family history. Mutations in superoxide dismutase-1 (SOD1) cause a rare form of familial ALS (fALS), and transgenic rodents expressing mutant human SOD1 (mutSOD1) capture many of the hallmarks of this fatal neurodegenerative disease, including the characteristic loss of motor neurons (MNs) (Kanning et al., 2010). Most of our current knowledge about the mechanisms of MN degeneration in ALS originates from studies in these fALS mouse models.

One clear conclusion from these studies is that nonneuronal cells play a critical role in mutSOD1-related neurodegeneration (Ilieva et al., 2009). We and others (Cassina et al., 2005; Di Giorgio et al., 2007; Nagai et al., 2007) have shown that astrocytes can provoke spontaneous degeneration of MNs. In particular, mutSOD1 mouse astrocytes trigger the death of both mouse primary and mouse embryonic stem-cell-derived MNs (mES-MNs), regardless of whether or not these neurons express pathogenic *SOD1* mutations (Nagai et al., 2007). Accordingly, mouse mutSOD1-expressing glial-restricted precursors grafted into spinal cords of wild-type (WT) rats produce a loss of neighboring MNs (Papadeas et al., 2011). These in vitro and in vivo studies demonstrate that mutSOD1-expressing astrocytes, but not other cell types, can induce MN degeneration. However, all of these findings were generated using cells from the mutSOD1 mouse. This is a potential issue both because levels of mutSOD1 are ~6-fold higher than those of the endogenous protein, and because of the uncertainty about what degree insights into human disease can be gained from murine models.

Subsequent studies have addressed some but not all of these concerns. Di Giorgio et al. (2008) and Marchetto et al. (2008) showed that both mouse mutSOD1-expressing astrocytes and human fetal astrocytes transduced to overexpress *SOD1* mutations cause loss of human ES-MNs (hES-MNs). Haidet-Phillips et al. (2011) reported that neural progenitor cell (NPC)-derived astrocytes generated postmortem from both sporadic and $fALS^{SOD1}$ patients were toxic for mES-MNs when cocultured, whereas NPC-astrocytes from a single non-ALS control were not toxic. However, it remains to be determined whether a non-cell-autonomous death phenotype would be observed in a fully humanized model of ALS.

The nature of the toxic activity mediated by astrocytes, and the mechanisms of MN death that they trigger, remain unclear even

in the rodent mutSOD1 systems, yet their identification has the potential to reveal new therapeutic targets. One candidate toxic factor in sALS was SOD1 itself, given that misfolded wtSOD1 is enriched in MNs of some sALS patients (Bosco et al., 2010; Guareschi et al., 2012). In keeping with this possibility, Haidet-Phillips et al. (2011) reported that silencing *SOD1* in hNPC-astrocytes from sALS patients (hence without SOD1 mutations) did attenuate the loss of mES-MNs.

Here, we have succeeded in creating a fully humanized in vitro model of ALS and show that astrocytes from sALS patients specifically kill hES-MNs, whereas control astrocytes do not. However, contrary to Haidet-Phillips et al. (2011), we show that silencing *SOD1* in human astrocytes from sALS patients (henceforth referred to as sALS astrocytes) does not mitigate MN toxicity. Instead, we found that MNs die in both the mouse mutSOD1 and the human sALS in vitro models by a caspase-independent form of programmed cell death (PCD) with necrotic morphology that closely resembles necroptosis, a form of programmed necrosis (Ofengeim and Yuan, 2013). Inhibition of this unique mechanism of non-cell-autonomous MN death represents a potential avenue for therapeutic investigations.

RESULTS

To closely model the human disease, we generated human adult astrocytes from sALS patients. Tissue samples were collected from motor cortex and, whenever possible, spinal cord within 11 hr of the time of death. The age-matched donors included six sALS patients (i.e., no family history of ALS or a mutation in any of the 27 familial ALS genes [see Supplemental Experimental Procedures available online]), 12 nonneurological controls comprising six nondisease controls (NDC) and six controls who died from respiratory failure due to chronic obstructive respiratory disorder (COPD), and three neurological controls with Alzheimer's disease (AD) (Figure S1A).

One day after plating, the human CNS cultures were composed predominantly of astrocytes and/or astrocyte precursors, as evidenced by ~90% of the cells being $CD44^+$, ~70% $vimentin^+$, and ~60% glial fibrillary acidic protein $(GFAP)^+$ (Figure S1B). By 7 days postplating, the proportions of $GFAP^+$ and $vimentin^+$ cells were essentially similar to those of the $CD44^+$ cells (Figure S1B). Conversely, the NPC markers SOX2 and PAX6 were not detected in three out of the four CNS cultures tested. In the one positive case, $SOX2^+/PAX6^+$ cells were observed only at 1 and 3 days postplating, and ~95% of those cells were $CD44^+$ and/or $GFAP^+$. Collectively, our data argue against the possibility that NPCs are major contributors to our human astrocyte cultures in contrast to those of Haidet-Phillips et al. (2011).

After 1 month postplating, the human CNS cultures became confluent, and cells maintained their CD44, vimentin, and GFAP expression patterns and displayed a star-like appearance with several fine processes (Figures 1A and S1C). These features were observed both in the NDC and the patient-derived COPD, AD, and sALS astrocytic cultures. In addition, other astrocyte markers as well as markers of immaturity/maturity and of reactivity did not differ among the four culture types or were not detected (Figure S1D). Furthermore, among a panel of 31 chemokines/cytokines, only a few were detected in the astrocyte culture media and, of these, only monocyte chemoattractant protein 1 (MCP1; gene *CCL2*) differed among the four groups (Figure S1D). As for other cellular components in the cultures, immunocytochemistry revealed no oligodendrocytes (2′,3′-cyclic-nucleotide 3′-phosphodiesterase [CNPase]), neurons (microtubule associated protein 2 [MAP2]), or microglia (ionized calcium binding adaptor molecule 1 [Iba1]) (Figure S1C). Likewise, quantitative RT-PCR (qRT-PCR) analysis indicated the absence of markers of oligodendocytes (myelin-associated glycoprotein [MAG]), neurons (synaptosomal-associated protein 25 [SNAP25]), microglia (Iba1), and endothelial cells (endothelial nitric oxide synthase [eNOS]) in all four groups of human CNS cultures.

To produce human spinal MNs, we differentiated the HUES3 *Hb9*::GFP reporter cell line (Di Giorgio et al., 2008), which expresses GFP under the control of the MN-specific *Hb9* promoter, using a protocol of early neuralization, retinoic acid caudalization, and sonic hedgehog agonist ventralization (Amoroso et al., 2013). Using this protocol, 20%–30% of the hES-derived neurons were GFP^+ MNs (Figure 1B). We confirmed that, like mES-MNs, hES-MNs were also susceptible, and to a similar degree (i.e., ~50% reduction in GFP^+ MNs at 7 days), to the toxicity of mouse mutSOD1 astrocytes (data not shown).

This result encouraged us to test the effects of sALS astrocytes on hES-MNs (Figures 1B–1F). Over a period of 14 days, the numbers of hES-MNs cultured on sALS astrocyte layers, but not those cultured on COPD and AD astrocytes, decreased substantially more than did those cultured on NDC astrocytes, reaching a plateau at day 7 (Figure 1G). Of note, at day 7 the difference in the numbers of GFP^+ neurons cultured on sALS versus control astrocytes was comparable to that of neurons immunostained for the MN marker nonphosphorylated neurofilament heavy chain (SMI32) or that of large neurons transduced with a viral vector expressing a *CMV::RFP*-reporter (Figure S1E). We thus conclude that the reduction in GFP^+ MN numbers reflect an actual loss of cells and not merely a loss of GFP expression.

To be considered predictive, any in vitro model of ALS needs to reproduce a cardinal feature of ALS, namely, selectivity for MNs. Survival at day 7 of non-MNs in mixed hES-derived cultures—as evidenced by counting both $MAP2^+/GFP^-$ non-MNs and $GABA^+/MAP2^+$ GABAergic interneurons—was not diminished by sALS as compared to control astrocytes (Figure 1H). Lastly, unlike astrocytes, primary fibroblasts from sALS patients did not cause any detectable reduction in hES-MNs compared to controls (Figure 1I). Non-cell-autonomous toxicity is therefore selective for MN-astrocyte interactions in human as in mouse.

Given the proposed roles for misfolded wtSOD1 as a cytotoxic factor even in sALS, we next explored the potential contribution of wtSOD1 to the toxicity of sALS astrocytes. Four lentiviral vectors, each expressing a different shRNA to human *SOD1*, were first tested in cells from our mutSOD1 mice, which express the G93A mutation found in human fALS patients. In infected and puromycin-selected primary mutSOD1 astrocytes, the shRNAs reduced SOD1 mRNA and protein by 50% to >75% (Figures S2B and S2C) and mitigated the toxicity of these astrocytes to mES-MNs (Figures 2A–2E).

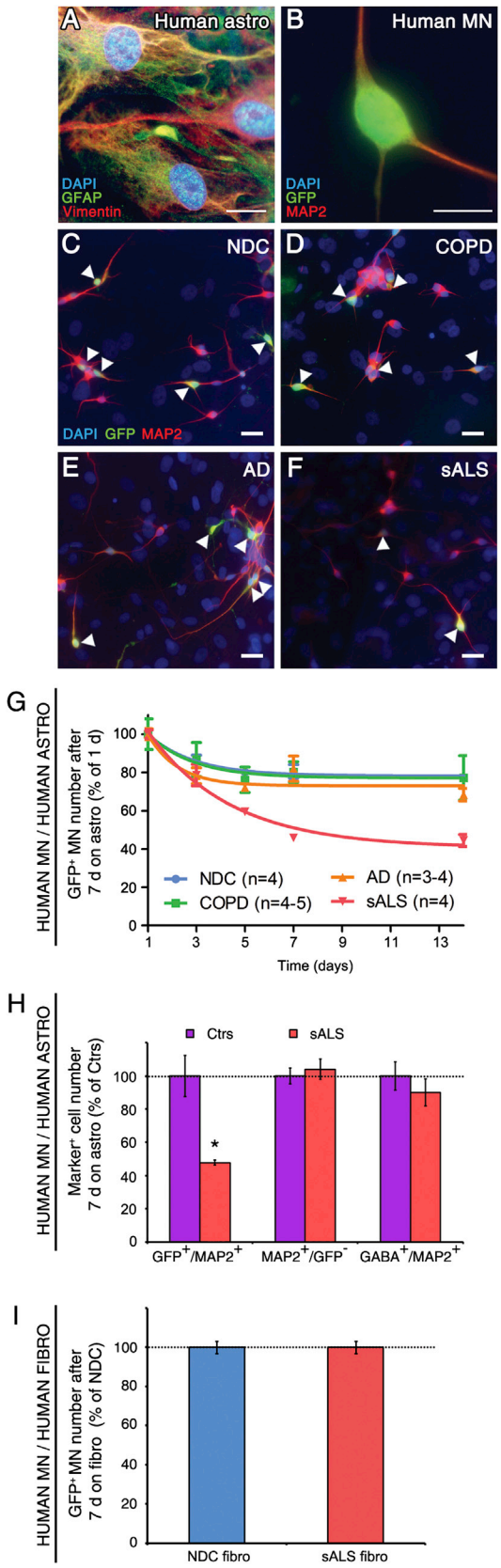

Figure 1. Primary Sporadic ALS Astrocytes Specifically Kill Human ES-MNs

(A) GFAP and vimentin immunostaining of primary astrocyte monolayers (astro) from sALS patients. (B) GFP and MAP2 immunostaining of hES-MN. (C–F) Representative images of hES-MNs cultured for 7 days on astro produced from NDC (C), COPD (D), AD (E), or sALS (F) subjects. White arrowheads indicate $GFP^+/MAP2^+$ MNs. (G) Quantification of hES-MN numbers over 14 days on NDC, COPD, AD, or sALS astro. Extra-sum-of-squares ANOVA (Bates and Watts, 1988) indicates that NDC, COPD, and AD curves do not differ ($F_{[3,33]} < 2.44$; $p > 0.075$) but that these curves are different from the sALS curve ($F_{[3,33]} > 19.12$, $p < 0.001$). (H) The number of $GFP^+/MAP2^+$ MNs is reduced when cocultured for 7 days with sALS astro compared to Ctrs astro (Ctrs = NDC, and/or COPD and/or AD) ($t_{[1,4]} = -5.5 \times 10^{-14}$, $p = 1.00$), but the number of non-MN neurons ($MAP2^+/GFP^-$ or $GABA^+/MAP2^+$) does not differ between the two conditions ($t_{[4]} = -0.523$, $p = 0.63$). (I) The number of hES-MNs is not different between cocultures with NDC or sALS fibroblasts after 7 days ($t_{[16]} = 0.023$, $p = 0.98$). Values represent means ± SEM (n = 3–9 per group). p values in (H) and (I) are from two-tailed unpaired Student's t tests. Scale bars represent 20 μm in (A) and (B) and 40 μm in (C)–(F).

We next tested these functionally validated SOD1 shRNAs on sALS astrocytes that carried no *SOD1* mutation. Knockdown of SOD1 mRNA in human cells with these four viral vectors was as effective or even more effective (clone 39808) as in mouse cells (Figures S2B and S2C), and the magnitude of reduction in SOD1 protein in human cells was more consistent across the four hairpins than in mouse cells (Figures S2B and S2C). Strikingly, however, the loss of hES-MNs caused by sALS astrocytes was not attenuated by *SOD1* silencing, regardless of whether the data were analyzed by individual shRNAs (Figures 2F–2J) or by individual patients (Figure S2D). Finally, silencing TAR DNA-binding protein 43 (TDP-43) in sALS astrocytes by 70%–80% (Figure S2D) also failed to mitigate hES-MN degeneration (Figure S2E). Thus, our results indicate that neither SOD1 nor TDP-43 contribute to sALS astrocyte toxicity.

To determine whether the mechanism by which sALS astrocytes are toxic to hES-MNs may be similar to that observed in the mouse mutSOD1 model (Nagai et al., 2007), we performed three experiments. First, in cocultures of sALS astrocytes with primary mouse spinal cord neuronal cultures, we found fewer mouse GFP^+-MNs (55% ± 6%), but no difference in $MAP2^+GFP^-$ non-MNs, 7 days after plating, compared to cocultures with control astrocytes (Figure 3A). Second, medium conditioned for 7 days with human sALS astrocytes phenocopied the selective toxicity of sALS astrocyte cells themselves to hES-MNs (Figure 3B). Finally, at day 3 in culture, a time point at which the number of hES-MNs is still ~85% of control, the proportions of hES-MNs displaying signs of DNA fragmentation (TUNEL assay), caspase-3 activation (fractin immunocytochemistry), or loss of plasma membrane integrity (ethidium homodimer [EthD] assay) were 2- to 4-fold higher in cocultures with sALS astrocytes as compared to control astrocytes (Figure 3C). These results are in keeping with those made previously in the mutSOD1 model (Nagai et al., 2007), and thus, both human sALS and mouse mutSOD1 astrocytes kill MNs probably via a soluble toxic factor that triggers a form of PCD with features of necrosis.

We sought to characterize further the mode of astrocyte-mediated MN death by performing, whenever possible, parallel studies in mouse and human MNs and with genetic and pharmacological interventions (Figure S3A). Given the critical role played

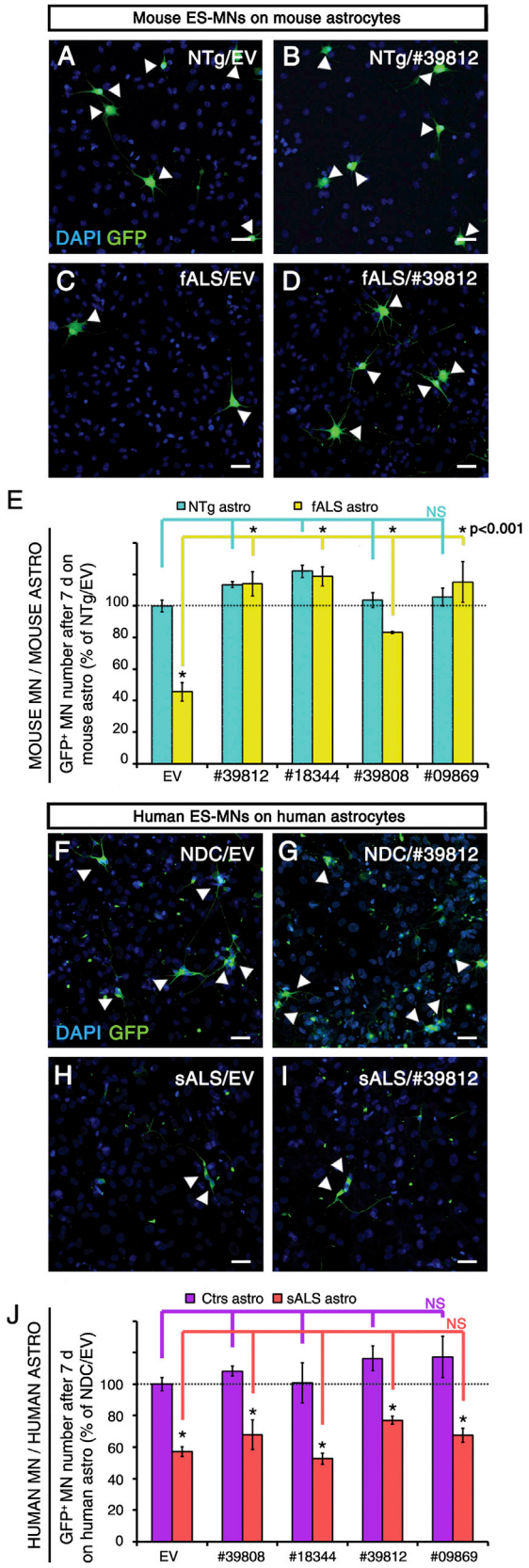

Figure 2. SOD1 Knockdown in Mouse, but Not in Human Astrocytes, Mitigates MN Loss

(A–D) Representative images of GFP$^+$ mES-MNs cultured for 7 days on mouse nontransgenic (NTg) astro infected with lentiviral empty vector (EV) (A) or a lentiviral shRNA hairpin (B) to knockdown human SOD1 (clone TRCN0000039812, 39812) or transgenic SOD1^{G93A} (fALS) astro infected with lentiviral EV (C) or lentiviral SOD1 shRNA 39812 (D). (E) Quantification of GFP$^+$ mES-MN number after 7 days on NTg or fALS astro infected with EV or one of the four shRNA clones against human SOD1 (39812, 18344, 39808, or 9869). GFP$^+$ mES-MN numbers on the fALS/EV astro are lower than on NTg/EV astro (*$p < 0.001$). However, GFP$^+$ mES-MN numbers on the fALS/shSOD1 astro are not different than those on the NTg/shSOD1 astro ($p > 0.05$). (F–I) Representative images of GFP$^+$ hES-MNs cultured for 7 days on astro prepared from NDC or sALS subjects. NDC astro were infected with EV (F) or the shRNA clone 39812 (G). sALS astro were also infected with EV (H) or clone 39182 (I). (J) Quantification of GFP$^+$ hES-MN number after 7 days on Ctrs or sALS astro infected with EV or one of the four shRNA clones. GFP$^+$ hES-MN numbers are lower when cocultured with sALS astro as compared to NDC astro under all lentiviral conditions (EV and shSOD1) (*$p < 0.001$). In addition, when compared within Ctrs or sALS conditions, GFP$^+$ hES-MN numbers are not different between EV- and shRNA-infected astro. (E and J) Data are expressed as percent of MN number on NTg or NDC astro infected with EV (percentage of NTg/EV or of NDC/EV) and represent means ± SEM (n = 3–9). p values in (E) and (J) are from post-ANOVA Newman-Keuls tests. (A–D and F–I) White arrowheads indicate GFP$^+$ MNs. Scale bars represent 40 μm.

by the Bcl-2 family in apoptosis, we first targeted the procell death protein Bax (Figure 3D). Bax$^{-/-}$ primary mouse MNs were resistant to mutSOD1 astrocyte toxicity (Figure S3B) and the pentapeptide Bax inhibitor V5 completely protected hES-MNs exposed to sALS astrocytes (Figure 3D). This effect was specific to Bax: neither Bak- nor Bim-deleted mouse primary MNs were more resistant to mutSOD1 astrocytes than their WT counterparts (Figure S3B). Moreover, inhibition of p53 by pifithrin-α or pifithrin-μ conferred no protection in either mouse or human systems (Figures S3C and S3D).

Caspases are the classical downstream effectors of Bax in the apoptotic pathway. However, although zVAD-fmk eliminated caspase-3 activation detected by fractin labeling in hES-MNs exposed to sALS astrocytes (Figure S3E), it did not increase the number of surviving MNs (Figure 3D), as we previously showed in mouse (Nagai et al., 2007). Moreover, zVAD-fmk did not reduce the fraction of EthD$^+$ or TUNEL$^+$ MNs in the human cultures (Figure S3E). Similarly, neither Ac-DNLD-CHO, which primarily inhibits the executioners caspase-3 and caspase-7, nor zIETD-fmk, a caspase-8 inhibitor, mitigated the MN loss in either the mouse (Figure S3C) or human (Figure S3D) coculture systems. Thus, MN death triggered by either fALS or sALS astrocytes is Bax dependent but caspase independent.

Necroptosis is a form of programmed necrosis that is not prevented by caspase inhibition (Ofengeim and Yuan, 2013) and is associated with loss of plasma membrane integrity (see EthD positivity in Figure 3C). We therefore targeted two key effectors of necroptosis, receptor-interacting serine/threonine-protein kinase 1 (RIP1) and mixed lineage kinase domain-like (MLKL) (Ofengeim and Yuan, 2013), in both mouse and human coculture systems. The RIP1 antagonist necrostatin-1 (Degterev et al., 2008) prevented the loss of ES-MNs exposed to either mutSOD1 or sALS (Figure 4A) astrocytes. Necrostatin-1 also reverted the proportions of EthD$^+$ and TUNEL$^+$ hES-MNs exposed to sALS astrocytes back to control levels (Figure 4B). In contrast,

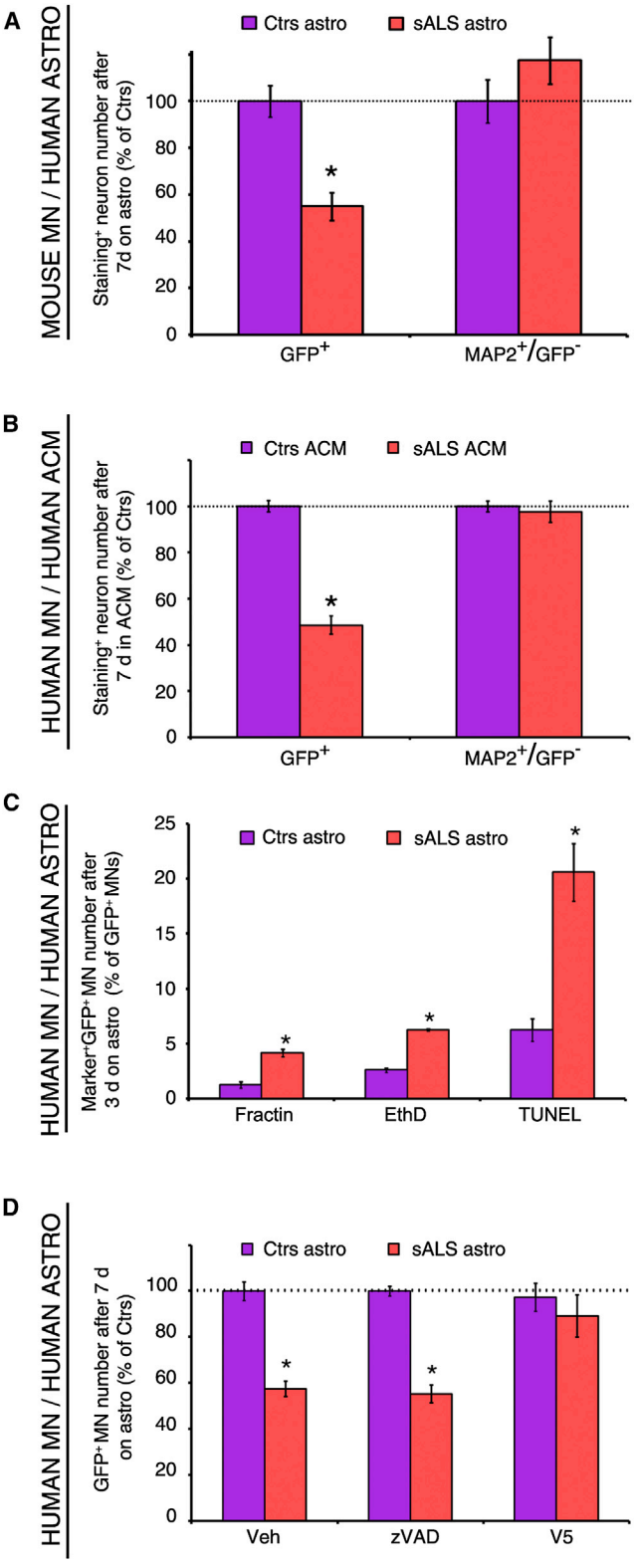

Figure 3. Human and Mouse Astrocytes Are Toxic through Similar Mechanisms

(A) Like hES-MNs (Figure 1H), mouse primary MN number is lower when cocultured with sALS astro as compared to Ctrs astro after 7 days (left, $t_{[22]}$ = 7.619, *p = 1.32 × 10^{-8}). In the same coculture wells, the number of non-MN neurons do not differ between sALS or Ctrs astro ($MAP2^+/GFP^-$, right, $t_{[17]}$ = −0.892, p = 0.385). (B) hES-MN number is lower when grown in media conditioned by sALS astrocytes as compared to Ctrs astrocytes (ACM) (left, *p < 0.001). Non-MN neuron numbers do not differ between these two conditions ($MAP2^+/GFP^-$, right, p = 0.626). (C) Numbers of hES-MNs fractin$^+$ (*p = 2.63 × 10^{-4}), $EthD^+$ (*p = 1.48 × 10^{-3}), or $TUNEL^+$ (*p = 9.11 × 10^{-4}) MNs are higher after 3-day exposure to sALS astro compared to Ctrs astro. (D) The reduction in hES-MN number when cocultured with sALS astro as compared to Ctrs astro (DMSO vehicle [Veh], *p < 0.001) is not mitigated by the addition of the pancaspase inhibitor zVAD-FMK (zVAD, 20 μM, *p < 0.001). Inhibition of Bax by the pentapeptide V5 (50 μM) abrogates the difference in hES-MN numbers when cocultured with sALS or Ctrs astro. Data are expressed as percent of MN or neuron number on Ctrs astro and represent means ± SEM (n = 4–7 per group). p values in (A) are from two-tailed unpaired Student's t tests and in (B)–(D) are from post-ANOVA Newman-Keuls tests.

necrostatin-1 did not alter caspase activation, since the proportion of fractin$^+$ ES-MNs in the human system remained unchanged (Figure 4B; data not shown for mouse). As an independent verification of the role of RIP1, mouse primary MNs were infected with a lentiviral vector expressing a RIP1 shRNA (22465) that reduced RIP1 levels in MNs by ~90% (Figure S4A). This knockdown provided nearly complete protection of mouse MNs exposed to mutSOD1 astrocytes (Figure 4C); comparable results were obtained with a second shRNA (22468; Figures S4A and S4B). Likewise, the silencing of RIP1 in hES-MNs by shRNA (200006; 60% reduction in human RIP1; Figure S4C) conferred complete protection against human sALS astrocyte toxicity (Figure 4D). In light of the discovery that MLKL can be specifically inhibited by necrosulfonamide (NSA) (Sun et al., 2012), we incubated our human cultures with this small molecule at a concentration of 0.25 μM. Under these conditions, NSA also reduced by ~90% the toxicity of sALS astrocytes for hES-MNs (Figure 4E). MN death triggered by toxic astrocytes from both familial and sporadic sources therefore bears the pharmacological hallmarks of necroptosis.

DISCUSSION

We report the development of a fully humanized in vitro model of sALS and its use to define a mechanism of MN degeneration. Primary adult astrocytes harvested from postmortem CNS tissues of sALS patients trigger degeneration of hES-MNs by the caspase-independent necroptosis pathway. This degeneration reflects many key hallmarks of ALS in vivo in human patients and mouse models. First, toxicity is only observed with ALS astrocytes and not with those from a series of other diseases or normal controls; albeit, we did not find any difference in the proportion of astrocytes or their degree of maturation among the four culture groups. Second, the toxicity is not linked to a heightened state of astrocyte reactivity. Third, it selectively affects MNs as compared to other neuronal classes. Lastly, another cell type from sALS patients, namely fibroblasts, does not exert MN toxicity. Using this validated system based on primary astrocytes, we excluded SOD1 itself as the toxic factor in sALS astrocytes. In contrast, our demonstration that the necroptosis pathway is required for astrocyte-triggered degeneration of MNs in both the human sALS and mouse

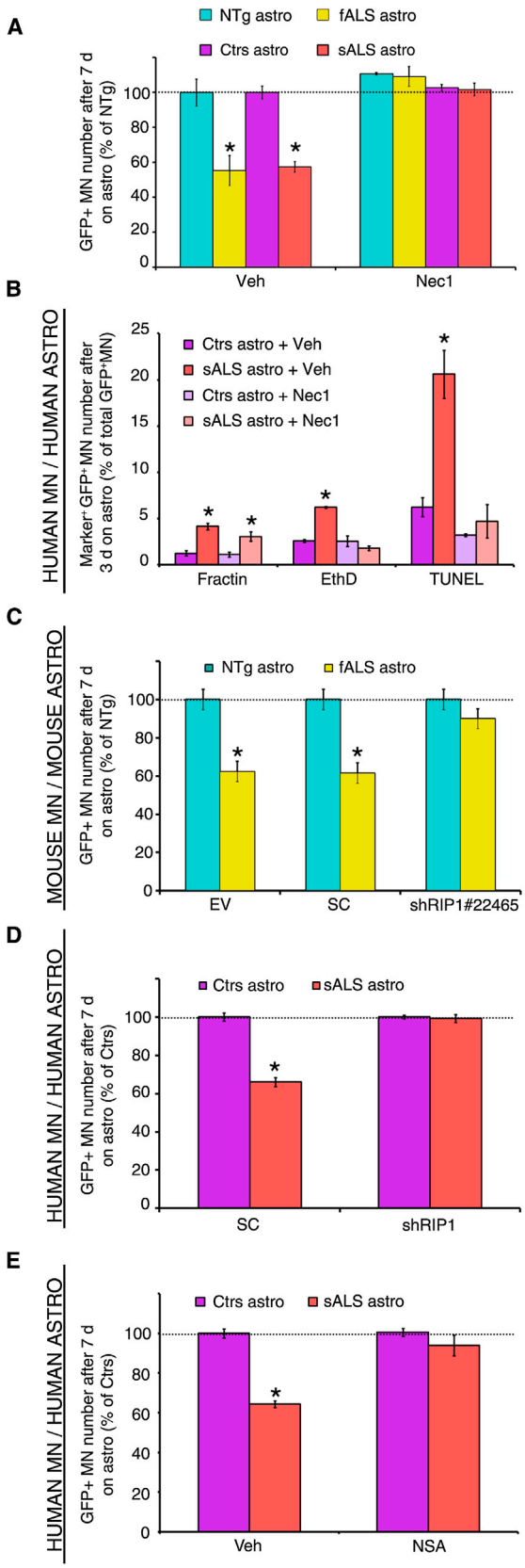

Figure 4. ALS Astrocytes Trigger Necroptosis in MNs, in an RIP1/MLKL-Dependent Manner

(A) Mouse primary or hES-MN MN number is reduced when cocultured for 7 days with fALS or sALS astro as compared to non-ALS astro (NTg, Ctrs) in the presence of vehicle (DMSO, *$p < 0.001$, left). The RIP1 inhibitor necrostatin-1 (Nec1, 5 μM) abrogates the MN loss observed in both mouse and human cocultures, respectively ($p = 0.532$, $p = 0.829$, right). (B) There are fewer TUNEL$^+$ and EthD$^+$ (*$p < 0.001$) hES-MNs but not fractin$^+$ ($p = 0.182$) MNs in sALS astro cocultures incubated with Nec1 compared to Veh. (C) There are more mouse primary MNs in cocultures with fALS astro where MNs are transduced with the viral vector containing the shRNA against RIP1 (22465) compared to EV or nonmammalian targeted scrambled (SC) transduced MNs (*$p < 0.001$). (D) There are more hES-MNs in cocultures with sALS astro where MNs are transduced with the viral vector containing the shRNA against RIP1 (200006) compared to EV-transduced hES-MNs (*$p < 0.001$). (E) In presence of Veh (DMSO), there are fewer (*$p < 0.001$) MNs on sALS astro compared to Ctrs astro. The loss of hES-MNs cocultured for 7 days on sALS astro is prevented by 250 nM of the MLKL inhibitor necrosulfonamide (NSA), as hES-MN numbers no longer differ ($p > 0.123$). Data are expressed as percent of MN number on Ctrs astro (A and E), or NTg astro (A), as percent of total MN population (B), or as percent of clone-transduced MN number on NTg astro (C and D) and represent means ± SEM (n = 3–5 per group). p values in (A)–(E) are from post-ANOVA Newman-Keuls tests.

fALS models opens the door to novel targeted therapeutic strategies.

How ALS astrocytes become toxic remains unclear. No known ALS-linked mutations were identified in our sALS samples and yet the toxic phenotype persisted even after several passages of the cultured adult astrocytes. Similarly, Haidet-Phillips et al. (2011) found that NPC-astrocytes from a patient with an *SOD1* mutation were toxic to MNs even after extensive expansion. In contrast, we have not found similar toxicity using induced pluripotent stem cell (iPSC)-derived astrocytes from patients with *SOD1* mutations (C. Henderson, personal communication). It seems therefore that some as-yet-unknown sALS-related imprinting in situ induces primary astrocytes to become and remain toxic. The lack of toxicity of astrocytes from control patients, and the fact that human sALS astrocytes do not show increased reactivity, suggests that toxicity does not result from generalized agonal hypoxia or a generic neuroinflammatory response. This implies the existence of a specific process underlying the gain of toxicity by human sALS astrocytes. Understanding the underlying epigenetic and genetic changes would shed considerable light on the progressive emergence of the ALS clinical phenotype.

Using our primary human sALS astrocyte/hES-MN coculture system, we found no evidence for a role of SOD1 in astrocyte toxicity. This is in contrast to the report from Haidet-Phillips et al. (2011) showing that knockdown of wtSOD1 protects mES-MNs against sALS NPC-astrocytes. How could this disparity be explained? Since we show that mouse and hES-MNs are equally susceptible to sALS astrocyte toxicity, the species origin of the MNs is not likely to explain the discrepancy. Our viral vectors led to the knockdown of human SOD1 protein by 50%–75%, comparable to the ~50% of protein reduction described to be effective in Haidet-Phillips et al. (2011), so differences in the magnitude of silencing also do not explain the divergent results. The puromycin selection on astrocytes cannot have masked a beneficial effect of silencing *SOD1* in sALS astrocytes since MN survival did not differ between

cocultures with nontreated astrocytes and EV-infected astrocytes treated with puromycin (Figure S2A). However, there were other technical differences. We used four different shRNAs targeting *SOD1*, none of which prevented astrocyte toxicity for MNs. One possibility is that the single shRNA hairpin used by Haidet-Phillips et al. (2011) caused off-target effects that led to a reduction in toxicity. Another difference is that our selection process generated cultures composed only of successfully transduced astrocytes and we systematically controlled for astrocyte density to exclude the possibility that a given shRNA might reduce astrocyte number and thereby affect toxicity indirectly. It is important to stress that our findings about the lack of SOD1 contribution only pertain to the non-cell-autonomous arm of ALS pathogenesis. The present study does not conflict with findings that misfolded wtSOD1 may contribute to MN degeneration by a cell-autonomous mechanism as proposed in several publications (Bosco et al., 2010; Guareschi et al., 2012).

Our observation that ES-MN death triggered by astrocytes was caspase independent and led to loss of plasma membrane integrity (i.e., EthD labeling) raised the possibility that the process was necrotic. These data alone did not exclude the possibility that upon caspase inhibition, MNs shift their form of PCD from apoptotic to nonapoptotic secondary necrosis (Krysko et al., 2006). However, we further found that inhibition of the key necroptosis effector RIP1 or MLKL, which plays a critical role in allowing the MLKL-RIP1-RIP3 necrosome complex to interact with downstream effectors (Ofengeim and Yuan, 2013), fully protected against sALS astrocyte-induced ES-MN death even in the absence of zVAD-fmk. This provided compelling evidence that necroptosis is the dominant mode of cell death in our in vitro model of sALS. Necroptosis has already been implicated in acute insults, such as brain ischemia (Degterev et al. 2005), but, to our knowledge, never before in a model of a neurodegenerative condition such as ALS. Tumor necrosis factor-α (TNF-α), Fas ligand (FasL), and TNF-related apoptosis-inducing ligand (TRAIL) are known to activate necroptosis upon ligation of their cognate receptors (Ofengeim and Yuan, 2013). However, none of these three agonists of necroptosis were detected by us in either mutSOD1 or sALS astrocyte-conditioned media (Nagai et al., 2007; Figure S1D; see Supplemental Information).

The signaling cascade downstream of RIP1 may provide a significant array of novel candidate therapeutic targets. The fact that MN death is dependent on Bax points to mitochondrial involvement, suggesting three potential mechanisms. Involvement of mitochondrial reactive oxygen species (Zhang et al., 2009) seems unlikely since neither the scavenger Mn-TBAP nor *N*-acetylcysteine protected MNs from mutSOD1-expressing astrocytes (D.B.R. et al., unpublished data). A second possibility is that mitochondria drive necroptosis via Bax-dependent permeabilization of the mitochondrial outer membrane, leading to the release of procell death factors such as AIF and subsequent DNA degradation and PCD (Artus et al., 2010). This might explain why the robust TUNEL signal that we observed (Figure 1I) was unexpectedly not reduced by zVAD-fmk. Third, at least in response to apoptotic signals, Bax can promote mitochondrial fission (Sheridan et al., 2008), which in turn can drive necroptosis through activation of dynamin-1-like protein by PGAM5 (Wang et al., 2012).

Our completely humanized cell model of sALS demonstrates that astrocyte-MN interactions are sufficient to trigger spontaneous neurodegeneration with many of the key aspects of the human disease. Our failure to find evidence of a role for SOD1 in our in vitro sALS model calls for a re-evaluation of the rationale of using therapeutic strategies aimed at reducing SOD1 expression in ALS patients other than those carrying *SOD1* mutations. However, our data do reveal a mechanism of non-cell-autonomous MN death, namely a Bax-sensitive form of necroptosis, whose inhibition represents a potential avenue for therapeutic intervention. The pathogenic significance of this molecular death pathway in ALS will have to be established in future studies by, for example, targeting RIP1 in in vivo models of the disease.

EXPERIMENTAL PROCEDURES

Only unpublished methods are described here; detailed methods can be found in the Supplemental Experimental Procedures. All the studies with human postmortem tissues were approved by Columbia IRB Committee protocol AAAA8153, ALS COSMOS Multicenter study IRB AAAD9986, and Columbia Coordinating Center IRB AAAC6618. The work performed with MNs derived from human embryonic stem cells has been approved by Columbia University ESCRO committee (Embryonic Stem Cell Research Oversight committee). Procedures related to in vitro experimentation with cells produced or derived from mice were approved by Columbia IACUC protocol AAAD8107.

Primary Cultures

Human astrocyte cultures were made as previously described by De Groot et al. (1997). Autopsied tissues were obtained from Columbia Medical Center Morgue or the National Disease Research Interchange (NDRI). The skin biopsies were performed after obtaining informed consent and fibroblasts were expanded and maintained under standard culture conditions in Medium 106 supplemented with LSGS (Life Technologies).

ES-Derived Neuron Cultures

Human spinal ES-MNs were derived as described previously (Amoroso et al., 2013).

Gene Silencing in Astrocytes and Motor Neurons

All shRNAs and EV used in this study were from Sigma MISSION. See Supplemental Experimental Procedures for details about the different hairpins. For astrocytes, a suspension of 100,000 cells/ml was treated with 8 μg/ml of hexadimethrine bromide (Sigma), exposed to lentiviral particles at an MOI of 15, centrifuged (800 × *g*, 30 min, room temperature), and plated (20,000 cells/well). After 48 hr, cells were selected by 1 μg/ml puromycin for 4.5 days and placed by in normal medium for 7 days before coculture with MNs. For both primary and ES-derived MNs, hexadimethrine bromide and puromycin were omitted.

SUPPLEMENTAL INFORMATION

Supplemental Information includes Supplemental Experimental Procedures and four figures and can be found with this article online at http://dx.doi.org/10.1016/j.neuron.2014.01.011.

ACKNOWLEDGMENTS

The authors acknowledge the help of Mr. Caicedo and Ms. Pradhan with the cell cultures, Mr. Hom, Mr. Garcia-Diaz, and Ms. Kim with hES-MNs, Dr. Jacquier with Metamorph, Dr. Crary for coordinating the procurement of human materials with the Columbia Morgue, Dr. Degterev for his input on necroptosis, and Dr. Jackson-Lewis and Dr. Schon with the manuscript preparation; the procurement of human tissues by the NDRI with the support of NIH grant 5 U42 RR006042; and the financial support from the NIH/NINDS

(NS062180, NS064191-01A1, NS042269-05A2, NS072182-01, NS062055-01A1, NS078614-01A1), the U.S. Department of Defense (W81XWH-08-1-0522 and W81XWH-12-1-0431), the NIEHS (ES009089), Project A.L.S., P2ALS, Target ALS, the ALS Association, the Muscular Dystrophy Association/Wings-over-Wall Street, the Parkinson's Disease Foundation, and A Midwinter Night's Dream. D.B.R. is recipient of a Career Development Award from the NIEHS Center of Northern Manhattan, V.L.V. of an Award for exchange programs between France and the United States from the Philippe Foundation, and K.P. of a TL1 Award TR000082-07 from NIH/NCATS. Skin biopsies were obtained as part of the ALS COSMOS project (R01ES160348). The artwork of Figure S3 was obtained through http://creativecommons.org/licenses/by/3.0/. L.H. is a student at Northport High School (Northport, NY 11768) and a recipient of the "A Midwinter Night's Dream" Summer Research Program scholarship.

Accepted: December 24, 2013
Published: February 6, 2014

REFERENCES

Amoroso, M.W., Croft, G.F., Williams, D.J., O'Keeffe, S., Carrasco, M.A., Davis, A.R., Roybon, L., Oakley, D.H., Maniatis, T., Henderson, C.E., and Wichterle, H. (2013). Accelerated high-yield generation of limb-innervating motor neurons from human stem cells. J. Neurosci. *33*, 574–586.

Artus, C., Boujrad, H., Bouharrour, A., Brunelle, M.-N., Hoos, S., Yuste, V.J., Lenormand, P., Rousselle, J.-C., Namane, A., England, P., et al. (2010). AIF promotes chromatinolysis and caspase-independent programmed necrosis by interacting with histone H2AX. EMBO J. *29*, 1585–1599.

Bates, D.M., and Watts, D.G. (1988). Nonlinear Regression Analysis and Its Applications. (Hoboken: John Wiley & Sons, Inc.).

Bosco, D.A., Morfini, G., Karabacak, N.M., Song, Y., Gros-Louis, F., Pasinelli, P., Goolsby, H., Fontaine, B.A., Lemay, N., McKenna-Yasek, D., et al. (2010). Wild-type and mutant SOD1 share an aberrant conformation and a common pathogenic pathway in ALS. Nat. Neurosci. *13*, 1396–1403.

Cassina, P., Pehar, M., Vargas, M.R., Castellanos, R., Barbeito, A.G., Estévez, A.G., Thompson, J.A., Beckman, J.S., and Barbeito, L. (2005). Astrocyte activation by fibroblast growth factor-1 and motor neuron apoptosis: implications for amyotrophic lateral sclerosis. J. Neurochem. *93*, 38–46.

De Groot, C.J., Langeveld, C.H., Jongenelen, C.A., Montagne, L., Van Der Valk, P., and Dijkstra, C.D. (1997). Establishment of human adult astrocyte cultures derived from postmortem multiple sclerosis and control brain and spinal cord regions: immunophenotypical and functional characterization. J. Neurosci. Res. *49*, 342–354.

Degterev, A., Huang, Z., Boyce, M., Li, Y., Jagtap, P., Mizushima, N., Cuny, G.D., Mitchison, T.J., Moskowitz, M.A., and Yuan, J. (2005). Chemical inhibitor of nonapoptotic cell death with therapeutic potential for ischemic brain injury. Nat. Chem. Biol. *1*, 112–119.

Degterev, A., Hitomi, J., Germscheid, M., Ch'en, I.L., Korkina, O., Teng, X., Abbott, D., Cuny, G.D., Yuan, C., Wagner, G., et al. (2008). Identification of RIP1 kinase as a specific cellular target of necrostatins. Nat. Chem. Biol. *4*, 313–321.

Di Giorgio, F.P., Carrasco, M.A., Siao, M.C., Maniatis, T., and Eggan, K. (2007). Non-cell autonomous effect of glia on motor neurons in an embryonic stem cell-based ALS model. Nat. Neurosci. *10*, 608–614.

Di Giorgio, F.P., Boulting, G.L., Bobrowicz, S., and Eggan, K.C. (2008). Human embryonic stem cell-derived motor neurons are sensitive to the toxic effect of glial cells carrying an ALS-causing mutation. Cell Stem Cell *3*, 637–648.

Guareschi, S., Cova, E., Cereda, C., Ceroni, M., Donetti, E., Bosco, D.A., Trotti, D., and Pasinelli, P. (2012). An over-oxidized form of superoxide dismutase found in sporadic amyotrophic lateral sclerosis with bulbar onset shares a toxic mechanism with mutant SOD1. Proc. Natl. Acad. Sci. USA *109*, 5074–5079.

Haidet-Phillips, A.M., Hester, M.E., Miranda, C.J., Meyer, K., Braun, L., Frakes, A., Song, S., Likhite, S., Murtha, M.J., Foust, K.D., et al. (2011). Astrocytes from familial and sporadic ALS patients are toxic to motor neurons. Nat. Biotechnol. *29*, 824–828.

Ilieva, H., Polymenidou, M., and Cleveland, D.W. (2009). Non-cell autonomous toxicity in neurodegenerative disorders: ALS and beyond. J. Cell Biol. *187*, 761–772.

Kanning, K.C., Kaplan, A., and Henderson, C.E. (2010). Motor neuron diversity in development and disease. Annu. Rev. Neurosci. *33*, 409–440.

Krysko, D.V., D'Herde, K., and Vandenabeele, P. (2006). Clearance of apoptotic and necrotic cells and its immunological consequences. Apoptosis *11*, 1709–1726.

Marchetto, M.C., Muotri, A.R., Mu, Y., Smith, A.M., Cezar, G.G., and Gage, F.H. (2008). Non-cell-autonomous effect of human SOD1 G37R astrocytes on motor neurons derived from human embryonic stem cells. Cell Stem Cell *3*, 649–657.

Nagai, M., Re, D.B., Nagata, T., Chalazonitis, A., Jessell, T.M., Wichterle, H., and Przedborski, S. (2007). Astrocytes expressing ALS-linked mutated SOD1 release factors selectively toxic to motor neurons. Nat. Neurosci. *10*, 615–622.

Ofengeim, D., and Yuan, J. (2013). Regulation of RIP1 kinase signalling at the crossroads of inflammation and cell death. Nat. Rev. Mol. Cell Biol. *14*, 727–736.

Papadeas, S.T., Kraig, S.E., O'Banion, C., Lepore, A.C., and Maragakis, N.J. (2011). Astrocytes carrying the superoxide dismutase 1 (SOD1G93A) mutation induce wild-type motor neuron degeneration in vivo. Proc. Natl. Acad. Sci. USA *108*, 17803–17808.

Sheridan, C., Delivani, P., Cullen, S.P., and Martin, S.J. (2008). Bax- or Bak-induced mitochondrial fission can be uncoupled from cytochrome C release. Mol. Cell *31*, 570–585.

Sun, L., Wang, H., Wang, Z., He, S., Chen, S., Liao, D., Wang, L., Yan, J., Liu, W., Lei, X., and Wang, X. (2012). Mixed lineage kinase domain-like protein mediates necrosis signaling downstream of RIP3 kinase. Cell *148*, 213–227.

Wang, Z., Jiang, H., Chen, S., Du, F., and Wang, X. (2012). The mitochondrial phosphatase PGAM5 functions at the convergence point of multiple necrotic death pathways. Cell *148*, 228–243.

Zhang, D.W., Shao, J., Lin, J., Zhang, N., Lu, B.J., Lin, S.C., Dong, M.Q., and Han, J. (2009). RIP3, an energy metabolism regulator that switches TNF-induced cell death from apoptosis to necrosis. Science *325*, 332–336.